Structure and thermotropic properties of 1-stearoyl-2-acetyl-phosphatidylcholine bilayer membranes

ARTICLE *in* BIOPHYSICAL JOURNAL · JUNE 1994

Impact Factor: 3.97 · DOI: 10.1016/S0006-3495(94)80937-3 · Source: PubMed

3 AUTHORS, INCLUDING:

Rick Duclos
Northeastern University
33 PUBLICATIONS **483** CITATIONS

SEE PROFILE

Structure and Thermotropic Properties of 1-Stearoyl-2-Acetyl-Phosphatidylcholine Bilayer Membranes

Jyotsna Shah, Richard I. Duclos, Jr., and G. Graham Shipley
Departments of Biophysics and Biochemistry, Boston University School of Medicine, Housman Medical Research Center, Boston, Massachusetts 02118 USA

ABSTRACT The structural and thermotropic properties of 1-stearoyl-2-acetyl-phosphatidylcholine (C(18):C(2)-PC) were studied as a function of hydration. A combination of differential scanning calorimetry and x-ray diffraction techniques have been used to investigate the phase behavior of C(18):C(2)-PC. At low hydration (e.g., 20% H_2O), the differential scanning calorimetry heating curve shows a single reversible endothermic transition at 44.6°C with transition enthalpy $\Delta H = 6.4$ kcal/mol. The x-ray diffraction pattern at −8°C shows a lamellar structure with a small bilayer periodicity $d = 46.3$ Å and two wide angle reflections at 4.3 and 3.95 Å, characteristic of a tilted chain, Lβ' bilayer gel structure. Above the main transition temperature, a liquid crystalline Lα phase is observed with $d = 53.3$ Å. Electron density profiles at 20% hydration suggest that C(18):C(2)-PC forms a fully interdigitated bilayer at −8°C and a noninterdigitated, liquid crystalline phase above its transition temperature ($T > T_m$). Between 30 and 50% hydration, on heating C(18):C(2)-PC converts from a highly ordered, fully interdigitated gel phase (Lβ') to a less ordered, interdigitated gel phase (Lβ), which on further heating converts to a noninterdigitated liquid crystalline Lα phase. However, the fully hydrated (>60% H_2O) C(18):C(2)-PC, after incubation at 0°C, displays three endothermic transitions at 8.9°C (transition I, $\Delta H = 1.6$ kcal/mol), 18.0°C (transition II), and 20.1°C (transition III, $\Delta H_{II+III} = 4.8$ kcal/mol). X-ray diffraction at −8°C again showed a lamellar gel phase (Lβ') with a small periodicity $d = 52.3$ Å. At 14°C a less ordered, lamellar gel phase (Lβ) is observed with $d = 60.5$ Å. However, above the transition III, a broad, diffuse reflection is observed at ≈39 Å, consistent with the presence of a micellar phase. The following scheme is proposed for structural changes of fully hydrated C(18):C(2)-PC, occurring with temperature: Lβ' (interdigitated) → Lβ (interdigitated) → Lα (noninterdigitated) → Micelles. Thus, at low temperature C(18):C(2)-PC forms a bilayer gel phase (Lβ') at all hydrations, whereas above the main transition temperature it forms a bilayer liquid crystalline phase Lα at low hydrations and a micellar phase at high hydrations (>60 wt% water).

INTRODUCTION

The lipid component of biological membranes is comprised of a heterogeneous mixture of different lipids such as phosphatidylcholines (PC), phosphatidylethanolamines (PE), sphingomyelins (SM), cerebrosides, cholesterol, etc. Some of these lipids form stable lamellar phases (e.g., PC and SM), and some other lipids form nonlamellar phases such as hexagonal (e.g., PE) or micellar (e.g., gangliosides and lysoPC) phases. Membrane lipid composition not only affects the possible structure the membrane adopts (Rand and Parsegian, 1989; Rand et al., 1990), it may also affect the properties (and consequently the function) of the membrane, notably its protein components. Lipids that promote the formation of nonlamellar structures have attracted much attention recently, mainly because of their possible role in membrane fusion and modulation of membrane protein activity (Hope et al., 1983; Eastman et al., 1992; Burger and Verkleij, 1990; Goldfine et al., 1987; Epand, 1987; Epand and Lester, 1990). The evaluation of the physical properties and the functional role of the individual lipids in the intact membrane requires an understanding of the dynamics of the various phases for a given system. Model systems consisting of either natural or synthetic lipids have been a valuable tool in obtaining basic information on membrane lipids.

Our previous work has been focused on studying the structural changes in hydrated mixed-chain phosphatidylcholines resulting from systematic reductions in the chain lengths of the fatty acids attached at the *sn*-1 and *sn*-2 positions. Using differential scanning calorimetry (DSC) and x-ray diffraction (Mattai et al., 1987; Shah et al., 1990), it has been shown that the chain length asymmetry greatly influences the packing properties of the hydrocarbon chains in the bilayer gel phase, and depending upon the degree of asymmetry, the lipids adopt noninterdigitated structures (e.g., C(18):C(18)-PC), partially-interdigitated phases (e.g., C(18):C(16)-PC), mixed-interdigitated phases (e.g., C(18):C(10)-PC), or fully interdigitated phases (e.g., C(18):C(0)-PC) to compensate for the chain length asymmetry (Huang and Mason, 1986; McIntosh et al., 1984; Hui et al., 1984; Mattai and Shipley, 1986; Mattai et al., 1987; Shah et al., 1990). However, above the main transition temperature highly asymmetric PCs (such as C(18):C(0)-PC and C(18):C(2)-PC), at high hydrations form a micellar phase (Mattai and Shipley, 1986; Huang et al. 1984), whereas other PCs (e.g., C(18):C(18)--PC, C(18):C(16)-PC, C(18):C(10)-PC) exist in a lamellar liquid crystalline phase (Huang and Mason, 1986).

The phase behavior of lysoPCs has been studied in detail using DSC, Raman, NMR, and x-ray diffraction techniques

Received for publication 9 September 1993 and in final form 31 January 1994.

Address reprint requests to G. Graham Shipley, Department of Biophysics, Housman Medical Research Center, Boston University School of Medicine, 80 East Concord Street, Boston MA 02118-2394. Tel.: 617-638-4009; Fax: 617-638-4041.

Abbreviations used: PC, phosphatidylcholine; PE, phosphatidylethanolamine; SM, sphingomyelin; DSC, differential scanning calorimetry.

0006-3495/94/05/1469/10 $2.00

(Reiss-Husson, 1967; Arvidson et al., 1985; Mattai and Shipley, 1986; Hui and Huang, 1986; Wu et al., 1982, 1984; Chang and Epand, 1983). These studies reveal that lysoPCs in excess water show a simple phase behavior. Below the transition temperature, these lipids form an interdigitated gel phase, and above the transition temperature a micellar phase exists at higher water content, and a hexagonal phase exists at lower water content. 1-stearoyl-2-acetyl-*sn*-glycerol-3-phosphocholine (C(18):C(2)-PC) is also structurally very asymmetrical (i.e., an 18 carbon chain at the *sn*-1 position and a 2 carbon chain at the *sn*-2 position). Earlier studies on C(18):C(2)-PC (Huang et al., 1984; Huang and Mason, 1986; Shah et al., 1990) show that C(18):C(2)-PC exhibits a complicated phase behavior in contrast to lysoPC (Mattai and Shipley, 1986; Hui and Huang, 1986). Based on the DSC data, Huang and Mason (1986) suggested that, on heating, C(18):C(2)-PC converts from a crystalline phase → gel (I) → gel (II) → micellar phase.

Two chemically synthesized phospholipids, 1-*O*-hexadecyl-2-acetyl-*sn*-glycero-3-phosphocholine (C(16)-PAF) and 1-*O*-octadecyl-2-acetyl-*sn*-glycero-3-phosphocholine (C(18)-PAF), exhibit similar phase behavior (Huang et al., 1986) with the interconversion between crystalline, gel, and micellar phases. C(18):C(2)-PC is of particular importance because it is a structural analog of platelet activating factor (PAF) and coexists with PAF upon the appropriate stimulation of a variety of cells (Satouchi et al., 1985, 1987). However, the structures of the phases formed by C(18):C(2)-PC have not been determined. We have examined the detailed structure and interconversions of different phases of C(18):C(2)-PC at various hydrations using a combination of DSC and x-ray diffraction techniques, to get an unambiguous picture of its phase behavior.

MATERIALS AND METHODS

C(18):C(0)-PC was obtained in lyophilized form (99% purity) from Avanti Polar Lipids (Alabaster, AL). Silica gel 60 analytical TLC plates were obtained from E. Merck (Darmstadt, Germany). Biosil A (100–200 mesh) was obtained from Biorad (Richmond, CA). Rexyn I-300 was obtained from Fisher (Fairlawn, NJ). Teflon membranes with 0.5-micron pores were obtained from Alltech (Deerfield, IL).

C(18):C(2)-PC synthesis

C(18):C(2)-PC had been prepared previously by Tence et al. (1981), Tokumura et al. (1981, 1985), Hirth and Barner (1982), Huang et al. (1984), and Shah et al. (1990). We prepared C(18):C(2)-PC by a variation of the reported methods (Gupta et al., 1977; Mason et al., 1981; Mangroo and Gerber, 1988; and Ali and Bittman, 1989) for the acylation of 1-acyl-*sn*-glycero-3-phosphocholines (lyso-PC). To a magnetically stirred solution of 100 mol % of C(18):C(0)-PC in 10 ml of alcohol-free anhydrous $CHCl_3$ under an atmosphere of argon was added 200 mol % of acetic anhydride dropwise over 1 min followed immediately by the addition of a solution of 200 mol % of freshly recrystallized 4-pyrrolidinopyridine (Patel and Sparrow, 1979) in 5 ml of $CHCl_3$. After 1 h, the reaction was complete by analytical TLC (silica gel 60, $CHCl_3$/MeOH/H_2O 60:30:4, C(18):C(0)-PC R_f = 0.05, C(18):C(2)-PC R_f = 0.09, duplicate plates and detection by both Molybdenum Blue Reagent according to Dittmer and Lester (1964), and cupric sulfate/phosphoric acid according to Bitman and Wood (1982)). The reaction mixture was concentrated by vacuum rotary evaporation and applied to a chromatographic column (Biosil A, $CHCl_3$) and eluted with a stepwise gradient of $CHCl_3$/MeOH/H_2O 60:30:0 to $CHCl_3$/MeOH/H_2O 60:30:4 to give the crude product. The white solid was dissolved in a minimum amount of $CHCl_3$/MeOH/H_2O 50:40:10 and filtered through a mixed-bed ion exchange column (Rexyn I-300, $CHCl_3$/MeOH/H_2O 50:40:10). The eluent was concentrated to give a white solid and was re-chromatographed (Biosil A, $CHCl_3$/MeOH 80:20) eluting stepwise with $CHCl_3$/MeOH 80:20 to $CHCl_3$/MeOH 20:80. The C(18):C(2)-PC eluted between $CHCl_3$/MeOH 50:50 and $CHCl_3$/MeOH 45:65. C(18):C(2)-PC was dissolved in $CHCl_3$ and filtered through a 0.5 micron teflon membrane, rotary evaporated, and dried for 48 h under high vacuum at 65°C in the presence of P_2O_5 to give pure C(18):C(2)-PC in 64% yield. Elemental analysis calculated for $C_{28}H_{58}NO_9P$: C, 57.61; H, 10.02; N, 2.20. Found: C, 57.92; H, 9.96; N, 2.08. The pure C(18):C(2)-PC melted at 244–246°C (softens at 235°C) showed a strong carbonyl stretch at 1735 cm^{-1}, and had a specific rotation of $[\alpha]_D^{25}$ +8° (c 1.0, $CHCl_3$/MeOH/H_2O 60:30:4 v:v:v) and $[\alpha]_D^{25}$ +7.0° (c 5.0, $CHCl_3$/MeOH 50:50 v:v), which compared favorably to the value of $[\alpha]_D^{20}$ +6.20 ± 0.06° (c 5.0, $CHCl_3$/MeOH 50:50 v:v) reported by Hirth and Barner (1982). The C(18):C(2)-PC was demonstrated to be 98 ± 1% pure containing 2% C(2):C(18)-PC from observing the acetyl methyl group singlet in the ^1H NMR ($CDCl_3$/CD_3OD 2:1 plus internal tetramethylsilane, C(18):C(2)-PC δ 2.09, C(2):C(18)-PC δ 2.07) and by ^{31}P NMR ($CDCl_3$/CH_3OH/H_2O 10:1:4 v:v:v plus internal *sn*-glycero3-phosphocholine δ −0.13), C(18):C(2)-PC δ −0.84, C(2):C(18)-PC δ −0.86) according to the method of Meneses and Glonek (1988).

Differential scanning calorimetry (DSC)

Hydrated multilamellar suspensions were prepared by a previously described method (Shah et al., 1990). Samples were stored at −4°C.

Calorimetric measurements were made with either a Perkin-Elmer (Norwalk, CT) DSC-2 or DSC-7 differential scanning calorimeter at a heating and cooling rate of 5°C/min. Data were analyzed by using a Perkin-Elmer Thermal Analysis Data Station (DSC-2) or Decstation personal work station (DSC-7), and transition enthalpies were calibrated by comparison with the gallium standard.

X-ray diffraction

Hydrated samples for x-ray diffraction studies were prepared by a method described elsewhere (Shah et al., 1990). X-ray diffraction patterns were recorded with photographic film using nickel-filtered Cu Kα radiation (λ = 1.5418 Å) from an Elliot GX-6 rotating anode generator (Elliott Automation, Borehamwood, U.K.). The x rays were focused into a point source using cameras with toroidal and double-mirror optics. The intensities of the diffraction lines were measured using an Automatic Recording Microdensitometer, Model MK III C. (Joyce-Loebl Ltd., Gateshead, England)

Starting with the bilayer periodicity (d), the values of lipid bilayer thickness (d_l), water layer thickness (d_f), and area (S) available to one lipid molecule were calculated using the following formulae (Luzzati et al., 1968):

$$d_l = d\left[1 + \frac{v_f}{v_l}\frac{1-C}{C}\right]^{-1} \qquad d_f = d - d_l \qquad S = \frac{2M_r v_l}{d_l(N \times 10^{-24})}$$

where v_f and v_l are the partial specific volumes of water and lipid, C is the lipid concentration, M_r is the molecular weight of the lipid, and N is Avogadro's number. At present, v_l values for mixed-chain PCs at either full hydration or at lower hydrations are not available. Thus, we have used values (calculated using the approach adopted by Tardieu et al., 1973) of 0.935 ml/g for the gel state and 1.00 ml/g for the liquid crystalline state. Similar values of v_l were used by McIntosh et al. (1984) in their study of C(18):C(10)-PC. These values of v_l are in good agreement with those determined by dilatometry for a series of saturated chain PCs in the gel and liquid crystalline states (Nagle and Wilkinson, 1978). The value of v_f is assumed to be 1.0 ml/g.

To calculate electron density profiles, the observed lamellar intensities $I(h)$ were corrected for the Lorentz factor (in our geometry and for unoriented samples this is $\alpha\ h^2$) giving $h^2I(h)$, and each hydration set was

normalized with respect to each other using the procedure described by Worthington and Blaurock (1969), i.e.,

$$\frac{2}{d} \sum h^2 I(h) = \text{constant}$$

The corresponding scaled, normalized structure amplitudes $F(s)$ are plotted as a function of reciprocal coordinate s ($s = 2 \sin \theta/\lambda$). Phasing of the lamellar reflections is done by inspection of the plotted amplitude data and by use of the Shannon sampling theorem (Shannon, 1949). The continuous amplitudes calculated for all phase combinations and the phase combination providing a satisfactory fit to all hydration amplitudes is selected. The distance between the two phosphate groups (d_{p-p}) is derived from the electron density profiles, which is an additional measure of bilayer thickness.[1]

RESULTS

Calorimetric studies of hydrated C(18):C(2)-PC

Representative DSC heating curves of C(18):C(2)-PC over the hydration range 10–80 wt% are shown in Fig. 1. On heating a 10% hydrated sample (from −10°C), a single sharp, reversible endothermic transition is observed at 53.7°C (ΔH = 6.4 kcal/mol). At 20% hydration, a relatively broad, asymmetric transition is observed at 44.6°C (ΔH = 6.4 kcal/mol). Further increases in hydration showed significant effects on the thermotropic behavior of C(18):C(2)-PC. Over the hydration range 30–50 wt% water, two endothermic transitions are observed; the two transition temperatures decrease on increasing hydration. At hydrations >60% water, three endothermic transitions are observed at 8.9, 18.0, and 20.1°C (transitions I, II, and III respectively). The enthalpy for transition I (T_m = 8.9°C) is 1.5 kcal/mol, and the combined enthalpy for the two higher temperature transitions (II and III) is 4.8 kcal/mol.

On cooling (data not shown), at 10% hydration, C(18):C(2)-PC shows essentially reversible behavior with a single exothermic transition at 49.0°C (ΔH = 6.8 kcal/mol). On increasing the hydration to 20%, the exothermic peak broadens and shifts to lower temperature (T_m = 33.0°C, ΔH = 6.9 kcal/mol). Further increases in the hydration (30–60 wt%) lead to the presence of multiple exothermic transitions with decreasing transition temperatures. However, at higher water contents (≥70%), no exothermic transition was observed on cooling from 30 to −5°C (Fig. 2, curve *b*).

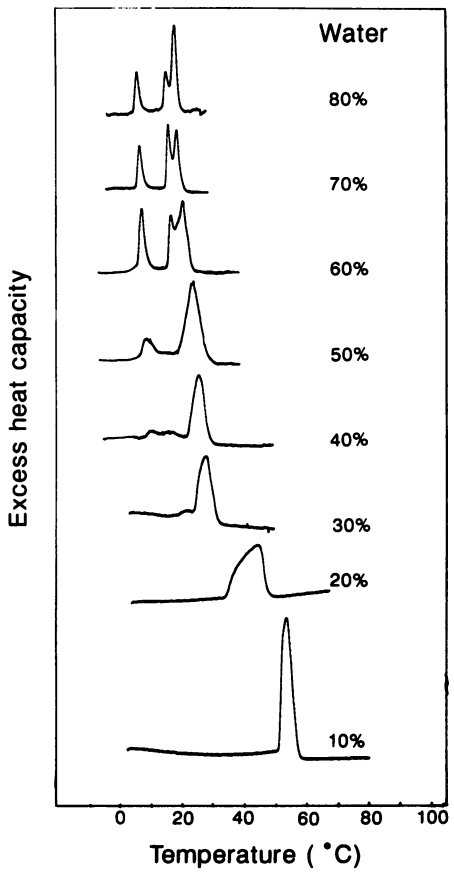

FIGURE 1 DSC heating scans of C(18):C(2)-PC at different hydrations (wt% water): DSC heating curves (heating rate 5°C/min) of C(18):C(2)-PC after incubation at 0°C for 1 h.

Kinetics of formation of low temperature gel phase(s) of 80% hydrated C(18):C(2)-PC

Fig. 2 (curve *a*) shows the DSC heating curve of C(18):C(2)-PC (80% water) after incubation for 1 h at 0°C. Three transitions are observed with transition I = 8.9°C (ΔH = 1.5 kcal/mol), transition II = 18.0°C, and transition III = 20.1°C (combined II+III, ΔH = 4.8 kcal/mol). On cooling from 30 to −5°C, no exothermic transition is observed (Fig. 2, curve *b*), and on immediate reheating no endothermic transition appears (Fig. 2, curve *c*). These data show that the low temperature phase (or phases) appears only after incubation at low temperature, thus indicating that these phases are generated in a temperature- and time-dependent manner. To determine the kinetics of formation of the low temperature phase(s), fully hydrated C(18):C(2)-PC was heated, cooled, and then incubated at different temperatures for different lengths of time.

Fig. 3 *A* shows the effect of incubation time (at 0°C) on the thermotropic behavior of fully hydrated C(18):C(2)-PC. The DSC heating scans of 80% hydrated C(18):C(2)-PC show (Fig. 3 *A*, curve *a*) that after 10-min incubation at 0°C, on heating two low enthalpy endothermic transitions appear at 8.9°C (ΔH = 0.3 kcal/mol) and at 19.0°C (ΔH = 0.13 kcal/mol). On increasing the incubation time, the enthalpies

[1] The d_{p-p} and d_l parameters do not provide the same measurement of lipid bilayer thickness. d_{p-p} is derived from the low resolution electron density profiles and measures the distance between the two electron dense phosphate groups located on each side of the bilayer. In contrast, d_l is calculated from the bilayer periodicity using the Luzzati formalism with the assumption that the lipid and water layers are discrete and that the partial specific volumes of both lipid and water remain unchanged as a function of hydration. Direct volumetric studies of phospholipids are rare, and volume data on less than fully hydrated lipid systems are even more difficult to obtain experimentally. In the absence of ν_l and ν_f values for C(18):C(2)-PC at any hydration or temperature, we have used a constant value of 0.935 ml/g for the gel state (see also, Nagle and Wilkinson, 1978).

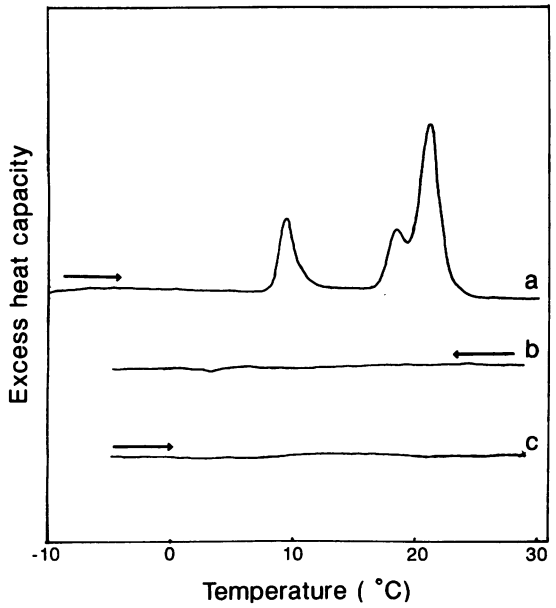

FIGURE 2 DSC heating scans of maximally hydrated C(18):C(2)-PC (80 wt% water) after low-temperature incubation: (*a*) Heating curve after 1-h incubation at 0°C; (*b*) cooling curve; and (*c*) immediate reheating curve. (Heating and cooling rate = 5°C/min.)

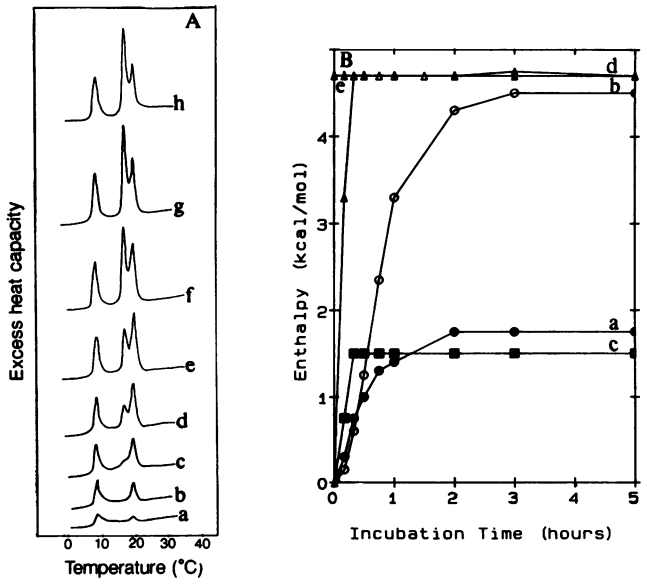

FIGURE 3 [*A*] DSC heating scans of fully hydrated C(18):C(2)-PC incubated at 0°C for different lengths of time: (*a*) 10 min; (*b*) 20 min; (*c*) 30 min; (*d*) 45 min; (*e*) 1 h; (*f*) 2 h; (*g*) 4 h; and (*h*) 20 h. [*B*] Dependence of enthalpies for different transitions on incubation time: (*a*) ΔH of low-temperature transition (I) on incubation at 0°C; (*b*) combined ΔH of high temperature transitions (II+III) on incubation at 0°C; (*c*) ΔH of low-temperature transition on incubation at −5°C; (*d*) combined ΔH of high-temperature transitions on incubation at −5°C; and (*e*) combined ΔH of high-temperature transitions on incubation at −10°C.

for both transitions increase (Fig. 3 *A*, curves *a–d*), and after 45-min incubation at 0°C, three endothermic transitions appear at 8.9, 18.0, and 20.1°C (Fig. 3 *A*, curve *d*). The enthalpy of the 8.9°C transition (I) and the combined enthalpy of two higher temperature transitions (II+III) increase with increasing incubation time reaching limiting values after approximately 2-h incubation (Fig. 3 *A*, curve *f*). However, the relative enthalpy of transition II compared to transition III increases with increasing incubation time (see Fig. 3 *A*, curves *d–h*). This ratio of the two enthalpies becomes constant after approximately 4-h incubation (see Fig. 3 *A*, curves *g* and *h*).

Fig. 3 *B* shows the kinetics of formation of the low temperature phase(s) at different temperatures. On incubation at 0°C, initially there is a slow increase in both enthalpies (I and II+III) with incubation time. On 10-min incubation the enthalpy for transition II+III increases from 0 to 0.13 kcal/mol, then the rate increases reaching a limiting value of 4.5 kcal/mol in approximately 2 h (Fig. 3 *B*, curve *b*). The enthalpy of transition I also follows a similar pattern and reaches a maximum value of 1.7 kcal/mol (Fig. 3 *B*, curve *a*) after 2 h; no further change was observed on longer incubation (up to 10 days). On lowering the incubation temperature to −5°C, the enthalpies of transition I as well as II+III, both reach their limiting values (1.5 and 4.7 kcal/mol respectively; Fig. 3 *B*, curves *c* and *d*) in only 10 min. On cooling the sample to −10°C, all three endothermic transitions appear with their maximum enthalpies on immediate reheating (i.e., without any incubation at −10°C; Fig. 3 *B*, curve *e*).

These results indicate that the formation of the low temperature phase(s) is highly temperature-dependent. Fig. 4 *A* shows the DSC heating curves of 80% hydrated C(18):C(2)-PC after supercooling to different temperatures (without incubation). Immediate reheating of C(18):C(2)-PC, cooled to −5°C, shows no endothermic transitions (Fig. 4 *A*, curve *a*; see also Fig. 3 *B*, curves *c* and *d*). On cooling to −6°C, a relatively broad endothermic transition at 11.1°C appears (Fig. 4 *A*, curve *b*); this transition increases in enthalpy on progressively lowering the cooling temperature to

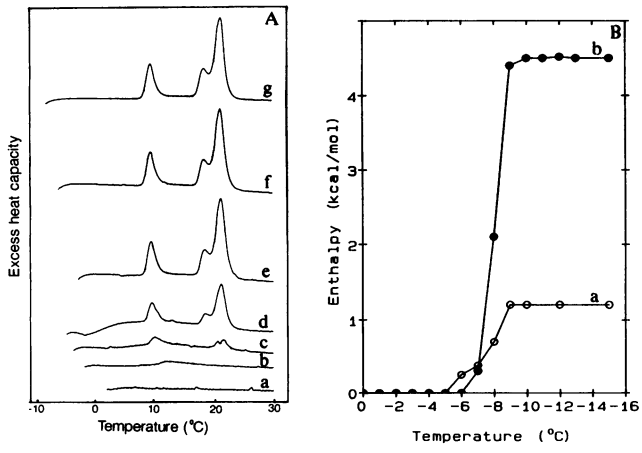

FIGURE 4 Effect of supercooling on the kinetics of the micellar → lamellar transition: fully hydrated C(18):C(2)-PC was cooled (5°C/min) to the specific temperatures and immediately reheated. [*A*] DSC heating scans of C(18):C(2)-PC after supercooling to different temperatures: (*a*) −5°C; (*b*) −6°C; (*c*) −7°C; (*d*) −8°C; (*e*) −9°C; (*f*) −10°C; and (*g*) −12°C. [*B*] Temperature dependence of transition enthalpies: (*a*) ΔH for transition I; and (*b*) combined ΔH for transitions II and III.

−9°C (Fig. 4 *A*, curves *c–e*) and then becomes constant at a value of 1.5 kcal/mol. On cooling to −7°C, the two higher temperature transitions II and III begin to appear (Fig. 4 *A*, curve *c*). The combined enthalpy for these transitions also increases on cooling to lower temperatures (Fig. 4 *A*, curves *c–e*), reaching a limiting value of ΔH = 4.5 kcal/mol (Fig. 4 *A*, curves *e–g*). Fig. 4 *B* shows the dependence of ΔH for these transitions on the supercooling temperature. These data reveal that on cooling to −6°C (Fig. 4 *A*, curve *b*), only transition I appears, and the higher temperature transitions appear only after cooling to −7°C or below (Fig. 4 *A*, curves *c–g*). This indicates, perhaps, that the high temperature phase (existing above transition III) converts directly to the low temperature phase (existing below transition I) and that the other intermediate phases can be formed by conversion from this low temperature phase.

Thus, the low temperature phase(s) can be formed either by incubating the sample at 0°C for long time periods (Fig. 3) or by supercooling the sample to −9°C or below (Fig. 4). However, a comparison of Figs. 3 *A* and 4 *A* reveals that the relative enthalpies of transitions II and III strongly depend on the low temperature incubation time, i.e., $\Delta H_{II}/\Delta H_{III}$ is the same irrespective of the supercooling temperature (Fig. 4 *A*), but the enthalpy ratio increases with low temperature incubation time (Fig. 3 *A*).

X-ray diffraction of hydrated C(18):C(2)-PC

To decipher the structures of the different phases, x-ray diffraction patterns of C(18):C(2)-PC have been obtained over the hydration range 10–80% water and at different temperatures. A representative x-ray diffraction pattern of a 20% hydrated sample of C(18):C(2)-PC is shown in Fig. 5. At −8°C, five low-angle reflections are observed (Fig. 5 *A*) corresponding to a bilayer periodicity, d = 46.3 Å. A sharp wide angle reflection at 4.3 Å is observed together with a broader reflection at 3.95 Å, characteristic of an ordered gel phase (Lβ') with tilted chain packing. These two reflections are present at all hydrations but with a small shift in position (see Figs. 5 *A* and 6 *A*). On increasing the hydration from 20 to 50 wt% water, the bilayer periodicity increases from 46.3 to 52.3 Å (see Fig. 7). On further increasing the hydration, no change in d (52.3 Å) is observed (Fig. 6 *A*).

At 53°C ($T > T_m$), for C(18):C(2)-PC (20% H_2O) a series of low-angle reflections corresponding to a bilayer periodicity of 53.3 Å are observed together with a single, diffuse wide angle reflection at 4.5 Å, indicative of a melted-chain Lα phase (Fig. 5 *B*). On increasing the hydration from 20 to 50 wt% water, the bilayer periodicity increases from 53.3 to 62.4 Å. The broad wide angle reflection at 4.5 Å is observed throughout the hydration range (10–80 wt% H_2O; for example, see Figs. 5 *B* and 6 *D*). Above 60% hydration, at $T > T_{III}$, the low angle diffraction pattern shows a single, broad, diffuse reflection at approximately 39 Å, indicating the presence of a micellar phase (Fig. 6 *D*). This suggests that for hydrations >60 wt% water, the high temperature phase is micellar (M).

As is obvious from the DSC heating scans (Fig. 1) and x-ray studies, at and below 20% hydration, only two phases (Lβ', below the transition temperature; and Lα, above the transition temperature) appear. However, at 30 wt% H_2O another phase starts appearing between the Lβ' and Lα phases, and apparently exists at all higher hydrations. To examine this phase, diffraction patterns of C(18):C(2)-PC, at 14°C, were recorded at 40, 50, 60, and 80% hydrations. The diffraction pattern at 80% hydration (Fig. 6 *B*) shows a series of low-angle reflections, typical of lamellar phases, corresponding to d = 60.5 Å. These lines are broader than those seen in the diffraction pattern at −8°C as is the single wide-angle reflection observed at 4.13 Å (compare Fig. 6, *A* and *B*), indicating a less ordered gel phase (Lβ). The bilayer periodicity of this phase increases from 53.2 to 60.5 Å, on increasing the hydration from 40 to 60 wt% water and remains constant thereafter (data not shown). To determine the structure of the phase existing between the transitions II and III, an x-ray diffraction pattern of C(18):C(2)-PC (80% water) was recorded at 19°C (Fig. 6 *C*). However, the diffraction pattern at this temperature was similar to that of the micellar phase (Fig. 6 *D*). This is probably because transition II and III are very close to each other; thus, at 19°C, it is difficult to get an isolated phase.

The bilayer periodicity d for C(18):C(2)-PC at −8°C is plotted as a function of water content in Fig. 7; d increases from 43.4 Å (10% water) to 52.3 Å (50% water) with no change observed on further increasing the water content. The

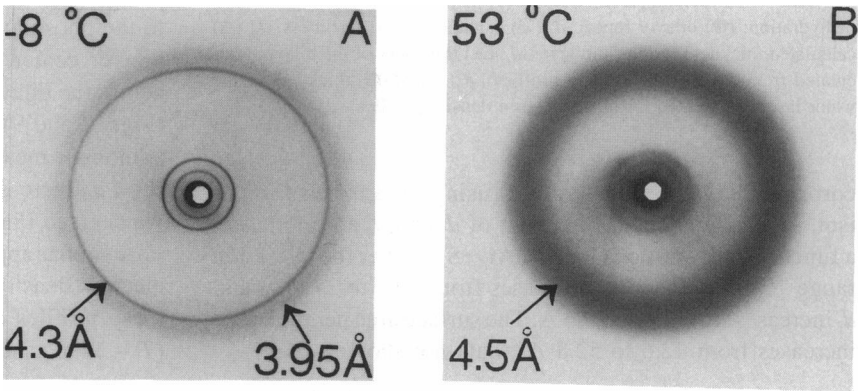

FIGURE 5 Representative x-ray diffraction patterns of 20% hydrated C(18):C(2)-PC: (*A*) at −8°C and (*B*) at 53°C.

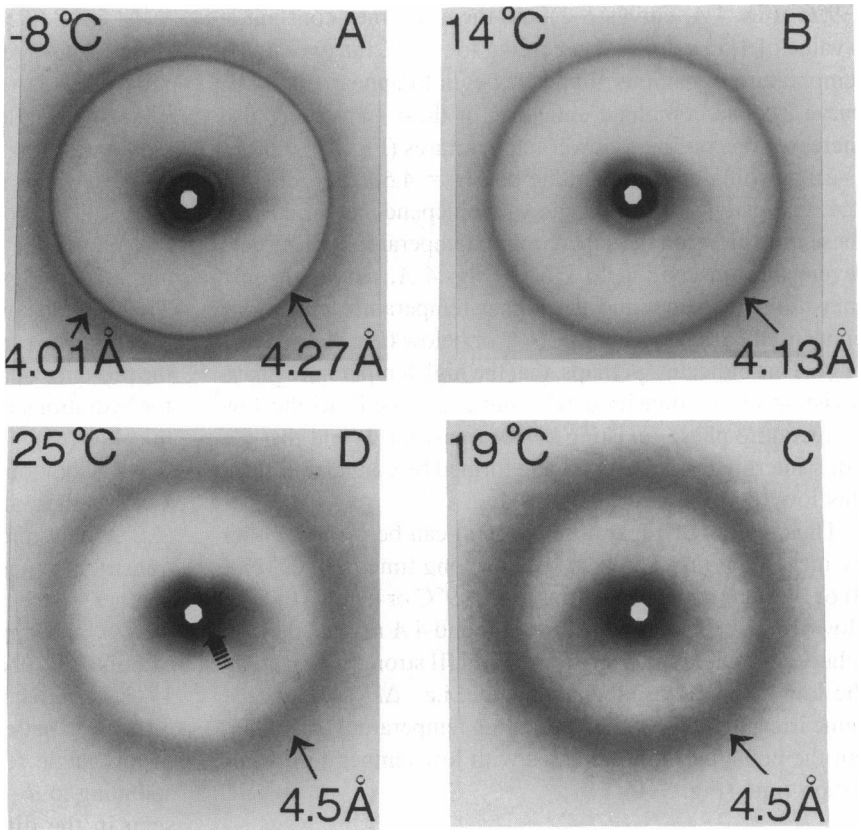

FIGURE 6 X-ray diffraction patterns of 80% hydrated C(18):C(2)-PC at: (*A*) −8°C, (*B*) 14°C, (*C*) 19°C, and (*D*) 25°C.

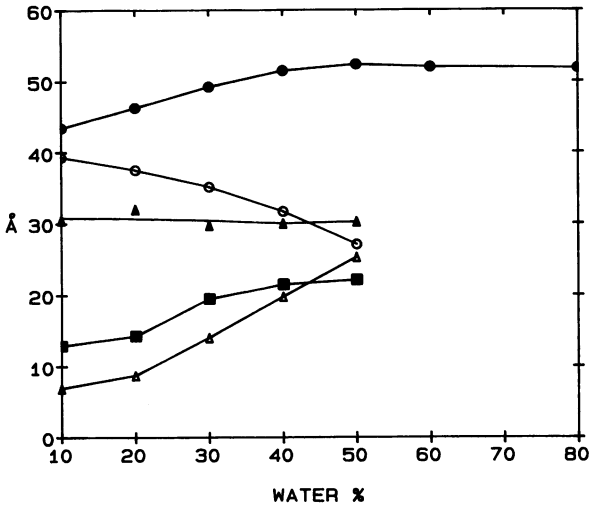

FIGURE 7 Structural parameters of C(18):C(2)-PC at −8°C as a function of hydration; (●) bilayer repeat, *d*; (○) calculated lipid thickness, d_l; (△) calculated thickness of the fluid layer, d_f; (▲) thickness of the bilayer (calculated from the electron density profiles), d_{p-p}; and (■) thickness of the water layer (calculated from the electron density profiles), d_w.

corresponding calculated values (using the Luzzati formalism, see Materials and Methods) of d_l and d_f are plotted as a function of hydration (Fig. 7). At −8°C, over the hydration range 10–50% water, d_l decreases from 39.3 to 27.0 Å, and d_f increases from 7.0 to 25.3 Å. The surface area per molecule increases from 42.6 to 52.8 Å^2 (data not shown).

To determine the electron density profiles for C(18):C(2)-PC at different hydrations, swelling experiments were carried out at −8°C, 14°C, and $T > T_m$ (depending upon the degree of hydration). For the phase at −8°C, Fig. 8 shows the structure factor amplitudes $F(s)$ plotted versus reciprocal co-ordinate s [$s = 2 \sin\theta/\lambda$] for the lamellar reflections recorded at 10, 20, 30, 40, and 50% hydration. The Shannon sampling theorem (Shannon, 1949; Sayre, 1952; King and Worthington, 1971; Torbet and Wilkins, 1976) was used to determine the correct phase combination for all hydration sets. The curve shown for the 20% hydration amplitudes identifies the nodes at $s = 0.013$, 0.052, 0.085, and 0.12 Å^{-1} where a change in phase angle (0 or π) could occur (Fig. 8), and the amplitudes were thus phased. The electron density profiles using reflections $h = 1$–5 were calculated based on these phases (Fig. 9). The profiles indicate a "bilayer" structure with the electron dense peaks at ±15.0 Å corresponding to the phosphorylcholine head groups, as well as a shallow bilayer center. At −8°C the head group separation, d_{p-p}, across the bilayer, remains constant at 30 Å at all hydrations (Figs. 7 and 9). The interlayer peak separation provides an additional measure of the water layer thickness $d_w = d - d_{p-p}$; d_w increases from 12.9 Å (10% water) to 22.1 Å (50% water) (see Fig. 7).

A similar approach (data not shown) was used to calculate electron density profiles at 14°C and at $T > T_m$. Examples of these profiles at various hydrations are shown in Fig. 10 ($T = 14$°C) and Fig. 11 ($T > T_m$). At 14°C, for all hydrations,

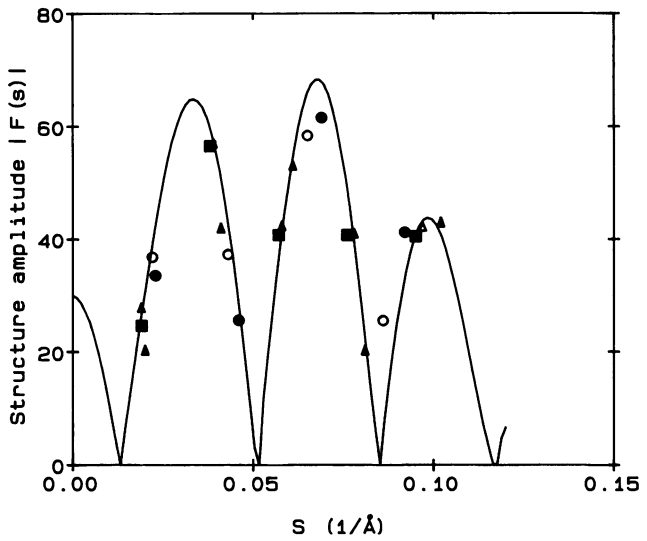

FIGURE 8 Structure amplitudes of C(18):C(2)-PC at −8°C for different hydrations: (●) 10% H_2O, (○) 20% H_2O, (▲) 30% H_2O, (△) 40% H_2O, and (■) 50% H_2O. Solid line is the theoretical curve calculated by using Shannon sampling theorem for 40% hydration.

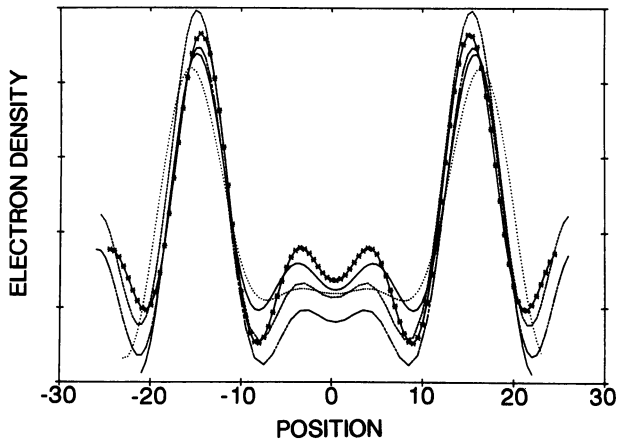

FIGURE 9 Electron density profiles of C(18):C(2)-PC at −8°C, at different hydrations; (*solid line*) 10% H_2O, (*dotted line*) 20% H_2O, (*asterisk line*) 30% H_2O, (*dashed line*) 40% H_2O, and (*dot-dash line*) 50% H_2O.

the electron density distribution across the bilayer center (calculated using reflections h = 1–3) shows a shallow trough.[2] From the location of the two electron-rich peaks at ±16.5 Å, the bilayer thickness, d_{p-p}, is essentially constant at 33 Å over the hydration range 40–60 wt% of water at 14°C (Fig. 10). At $T > T_m$, the electron density profiles calculated for h = 1–4 show two peaks at ± 20.5 Å corresponding to a bilayer thickness d_{p-p} of 41.0 Å, and the center shows a

[2] The use of only three structure factors increases the series termination error problem in the Fourier summation, notably at the bilayer center and a shallow trough is observed (see Fig. 10). However, the presence of the two electron dense peaks at ±16.5 Å indicates strongly that the phase present at 14°C remains interdigitated.

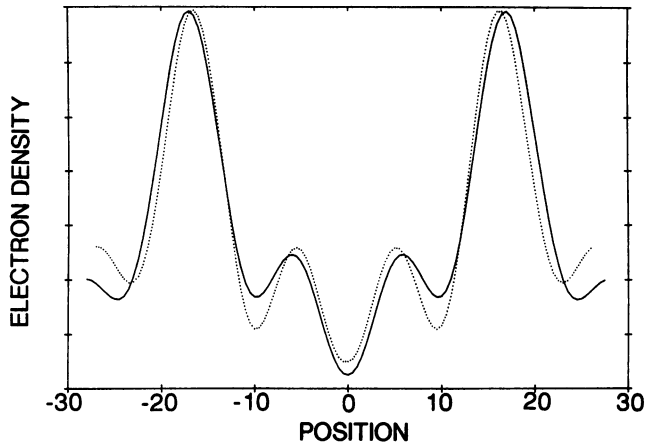

FIGURE 10 Electron density profiles of C(18):C(2)-PC at 14°C for (*dotted line*) 40% H_2O and (*solid line*) 50% H_2O.

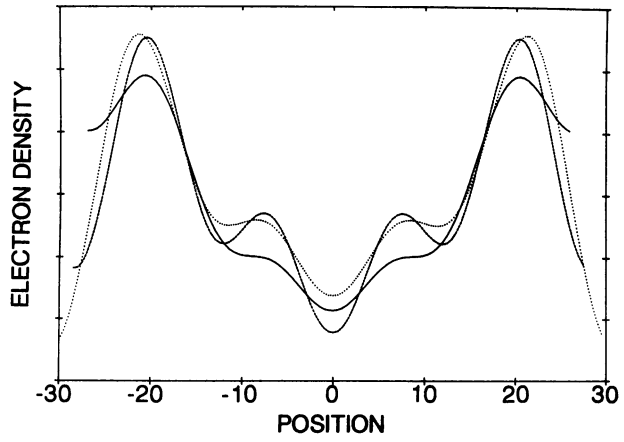

FIGURE 11 Electron density profiles of C(18):C(2)-PC at $T > T_m$ for various different hydrations: (*solid line*) 20% H_2O, (*dashed line*) 30% H_2O, and (*dotted line*) 40% H_2O.

pronounced trough indicative of a classic bilayer structure. The bilayer thickness remains constant throughout the hydration range, 10–50 wt% water. Thus, the lipid layer thickness, d_{p-p} is greater for the liquid crystalline state (41.0 Å) than for gel state (30.0 or 33.0 Å). The head group surface area per molecule varies from 42.5 to 48.4 Å^2 over the hydration range 10–40 wt% water.

DISCUSSION

The calorimetric studies of C(18):C(2)-PC show that the thermotropic properties of the lipid change with hydration. The DSC scans show that below 30% hydration, only a single thermal transition appears indicative of presence of two phases. Between 30 and 50 wt% H_2O, two endothermic transitions (three phases) appear, and above 60% H_2O, three endothermic transitions (four phases) are present. Above 60% hydration, at 30°C (above transition III) the preparation is optically clear, which, together with the x-ray diffraction data

(Fig. 6 *D*), indicates the presence of a micellar phase. However, below transition I a well ordered, interdigitated lamellar gel phase (Lβ') exists (see Figs. 5 *A* and 6 *A*). The kinetics of the micellar → lamellar transition of fully hydrated C(18):C(2)-PC at 0°C show that after an initial slow nucleation process (Zettlemoyer, 1969; Wu and Huang, 1983; Mattai and Shipley, 1986), the phase change is completed in about 2 h (Fig. 3, *A* and *B*). However, faster kinetics are observed on cooling to −5°C, the micellar → lamellar transition being completed in approximately 10 min. On cooling to −10°C, this process is completed instantly. On supercooling, initially the Lβ' phase forms. On heating other phases start appearing. This indicates that C(18):C(2)-PC is rearranged from a dynamic micellar phase to a stable interdigitated gel phase (Lβ'), and this phase then converts into another lamellar gel phase (Lβ).

Our x-ray diffraction data for the low temperature phase of C(18):C(2)-PC, at −8°C, show a lamellar phase. The wide-angle reflections at 4.3 and 3.95 Å, suggest that the hydrocarbon chains are tilted with respect to the bilayer normal. This Lβ' phase swells to a maximum at approximately 40% H_2O corresponding to approximately 21 molecules of water "bound" per molecule of C(18):C(2)-PC molecule. The short lipid layer thickness of 30 Å (compared to that of C(18):C(18)-PC) and the absence of a well defined central trough in the electron density profiles (Fig. 9) indicate that the hydrocarbon chains are packed in a fully interdigitated mode in which the 18-carbon chain of one C(18):C(2)-PC molecule extends across the bilayer and lies against the 2-carbon chain of the another PC molecule in the opposing leaflet (see Fig. 12). A similar interdigitated, tilted chain structure has been reported for the low-temperature phase of C(18):C(0)-PC (Mattai and Shipley, 1986).

The low angle x-ray diffraction data for the second phase, present in >30% H_2O at 14°C, show a less ordered lamellar gel phase (Lβ). The single wide-angle reflection at 4.13 Å indicates that the chains are packed in a hexagonal array (Fig. 6 *B*). The electron density profiles (Fig. 10) show a relatively short phosphate-phosphate distance of 33 Å (although slightly larger than that of Lβ' phase) and a shallow bilayer center. Again, this indicates an interdigitated chain packing. The phosphate-phosphate distance of 37.5 Å is calculated for an untilted interdigitated structure assuming that the hydrocarbon chains are rigid and in an all-*trans* configuration. Because the experimental d_{p-p} for the Lβ' and Lβ phases are 30 and 33 Å respectively, the angle of tilt for the Lβ' and Lβ phases are calculated to be 37 and 28°, respectively.

The x-ray diffraction data of C(18):C(2)-PC, for 20% hydration at 53°C, show a conventional lamellar liquid crystalline L_α phase (Fig. 5 *B*). The electron density profiles for this phase show a much larger phosphate-phosphate distance of 41 Å (note that in conventional bilayers, the lipid layer thickness in the gel phase is usually larger than the lipid layer thickness in the liquid crystalline phase), and a well defined central trough is observed (Fig. 11). Both the larger d_{p-p} and the sharp central trough suggest a noninterdigitated chain packing for the liquid crystalline phase. As shown in Fig. 12,

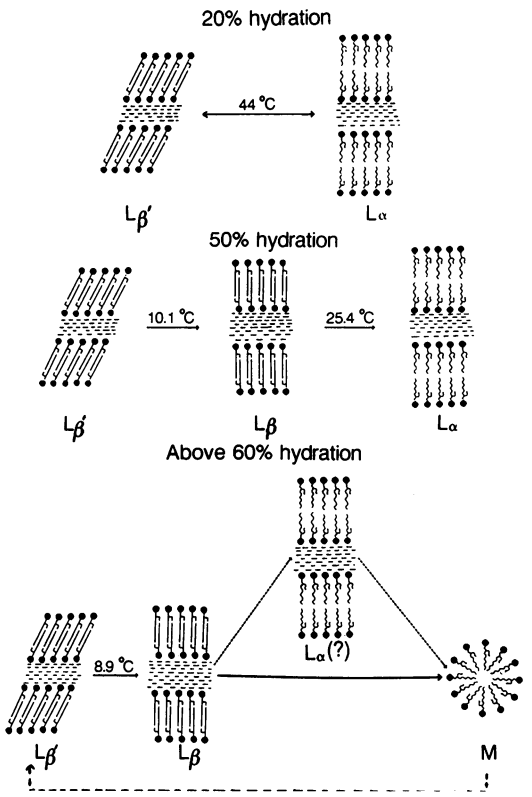

FIGURE 12 Summary of the phase behavior of C(18):C(2)-PC.

this phase corresponds to a packing where the melted C(18)-acyl chain of one C(18):C(2)-PC molecule lies against the C(18)-acyl chain of another C(18):C(2)-PC molecule from the opposing layer of the bilayer, and the short C(2)-acyl chain is somehow accommodated. This phase can be detected clearly from 10 to 50% hydration. However, at and above 60% hydration, instead of this gel to liquid crystalline phase transition, there are two endothermic transitions at 18.0°C (transition II) and 20.1°C (transition III). According to the DSC studies by Huang et al. (1986), the transition at 18.0°C is reported as a pretransition. Because these transition temperatures are very close to each other, due to experimental limitations, it is impossible to get a well resolved x-ray diffraction pattern in between these transitions (Fig. 6 *C*). The similar bilayer periodicity for the Lβ and Lα phases at full hydration further complicates the situation.

However, based on the hydration studies, we suggest that the transition II corresponds to a gel (Lβ) to liquid crystalline Lα phase transition. In this Lα phase (as is obvious from its structure; see Fig. 12), the hydrocarbon center of C(18):C-(2)-PC is highly disordered. This disorder probably imposes instability to the C(18):C(2)-PC lamellar phase and thus facilitates a breakdown of these lamellar bilayers into micelles (Fig. 12) in excess water. Consequently, above 60% hydration only a micellar phase is observed above the transition III. This is supported by the x-ray diffraction pattern of C(18):C(2)-PC in excess water, at $T > T_{III}$ (Fig. 6 *D*). However, the observed enthalpy of transition III is much higher than expected for a liquid crystalline → micelle transition (Fig. 2,

curve *a*). This may be explained on the basis of inhomogeneous nucleation and growth of the lamellar sheets (Zettlemoyer, 1969; Wu and Huang, 1983; Mattai and Shipley, 1986). On supercooling the enthalpy of transition II remains lower than transition III irrespective of the supercooling temperature (Fig. 4 *A*). However, on incubation at 0°C, initially the enthalpy of transition II is lower than transition III. But after a 4 h incubation the enthalpy of transition II is larger than that of transition III (Fig. 3 *A*, curves *g* and *h*). This suggests that supercooling to −9°C is sufficient to start the nucleation process of the small lamellar sheets, but the incubation facilitates the formation of the large lamellar sheets. Probably the small lamellar vesicles or sheets are capable of converting directly to micelles (perhaps giving rise to transition III), and the large lamellar sheets (similar to the lamellar sheets existing at low hydration) may convert to the Lα phase (perhaps giving rise to transition II), which eventually converts to the micellar phase (perhaps also contributing to transition III).

A summary of the structural changes occurring in C(18):C(2)-PC with temperature and hydration is given in Fig. 12. At ≤20% hydration, C(18):C(2)-PC converts from a fully interdigitated gel phase (Lβ') to a noninterdigitated liquid crystalline Lα phase. This is a completely reversible process. Between 30 and 50% hydration, three phases are observed. At low temperature a fully interdigitated, tilted chain gel phase (Lβ') is formed which, on heating, converts to a less ordered, fully interdigitated lamellar gel phase (Lβ). On further increasing the temperature, this lamellar gel phase (Lβ) converts to a noninterdigitated liquid crystalline Lα phase (Fig. 12). However, fully hydrated (>60% hydration) C(18):C(2)-PC shows a systematic conversion from a well ordered interdigitated gel phase (Lβ') to a less ordered interdigitated gel phase (Lβ). Depending on the previous history of the sample, this phase may convert directly to a micellar phase (L$\beta \rightarrow$ M) or may convert to a noninterdigitated liquid crystalline (L$\beta \rightarrow$ Lα) phase, and then eventually convert to the micelles (L$\beta \rightarrow$ L$\alpha \rightarrow$ M). On supercooling or long incubation at 0°C, this micellar phase can be converted to the interdigitated gel phase (M $\rightarrow$ Lβ').

A comparison of C(18):C(0)-PC and C(18):C(2)-PC shows that, although both the lipids are highly asymmetric, in excess water C(18):C(0)-PC shows a simple behavior with the interconversion of the gel and micellar phases. On the other hand, C(18):C(2)-PC exhibits a very complex behavior. Although there is no structural basis to explain the difference in the behavior of C(18):C(2)-PC and C(18):C(0)-PC in excess water, it is reasonable to assume that in lyso-PC, the hydroxyl group at the *sn*-2 position is participating in intermolecular hydrogen bonding that may favor the formation of extended lamellar sheets—stable bilayers at low temperatures. At high temperature these hydrogen bonds weaken, and the C(18):C(0)-PC interdigitated bilayer breaks down into micelles. In C(18):C(2)-PC, the acetyl group at the *sn*-2 position may also cause some packing perturbations in the interfacial region in addition to reducing the hydrogen bonding possibilities. Although the presence of the acetyl group does not seem to affect the interdigitation process during conversion from the micellar to the lamellar phase on cooling, it may inhibit the growth of the stable lamellar sheets (even after long incubations at low temperatures) characteristic of C(18):C(0)-PC. The less stable interdigitated lamellar gel phase of C(18):C(2)-PC may convert, on heating, to other lamellar phases before bilayer disruption/micelle formation occurs.

We thank Mr. J. Owusu-Djambo for the technical help and Dr. D. Atkinson for valuable advice. This research is supported by research grant HL 26335 from the National Institutes of Health.

REFERENCES

Ali, S., and R. Bittman. 1989. Mixed-chain phosphatidylcholine analogues modified in the choline moiety: preparation of isomerically pure phospholipids with bulky head groups and one acyl chain twice as long as the other. *Chem. Phys. Lipids.* 50:11–21.

Arvidson, G., I. Brental, A. Khan, G. Lindblom, and K. Fontell. 1985. Phase equilibria in four lysophosphatidylcholine/water systems: exceptional behavior of 1-palmitoyl-glycerophosphocholine. *Eur. J. Biochem.* 152: 753–759.

Bitman, J., and D. L. Wood. 1982. An improved copper reagent for quantitative densitometric thin-layer chromatography of lipids. *J. Liquid Chromat.* 5:1155–1162.

Burger, K. N. J., and A. J. Verkleij. 1990. Membrane fusion. *Experientia.* 46:631–644.

Chang, H., and R. M. Epand. 1983. The existence of a highly ordered phase in fully hydrated dilauroylphosphatidyl-ethanolamine. *Biochim. Biophys. Acta.* 728:319–324.

Dittmer, J. C., and R. L. Lester. 1964. A simple, specific spray for the detection of the phospholipids on thin-layer chromatograms. *J. Lipid Res.* 5:126–127.

Eastman, S. J., M. J. Hope, K. F. Wong, and P. R. Cullis. 1992. Influence of phospholipid asymmetry on fusion between large unilamellar vesicles. *Biochemistry.* 31:4262–4268.

Epand, R. M. 1987. The relationship between the effects of drugs on bilayer stability and on protein kinase C. *Chem. Biol. Interact.* 63:239–247.

Epand, R. M., and D. S. Lester. 1990. The role of membrane biophysical properties in the regulation of protein kinase C activity. *Trends Pharmacol. Sci.* 11:317–320.

Goldfine, H., N. C. Johnston, J. Mattai, and G. G. Shipley. 1987. Regulation of bilayer stability in Clostridium butyricum: studies on the polymorphic phase behavior of the ether lipids. *Biochemistry.* 26:2814–2822.

Gupta, C. M., R. Radhakrishnan, and H. G. Khorana. 1977. Glycerophospholipid synthesis: Improved general method and new analogs containing photoactivable groups. *Proc. Natl. Acad. Sci. USA.* 74:4315–4319.

Hirth, G., and R. Barner. 1982. Preparation of 1-O-octadecyl-2-O-acetyl-sn-glyceryl-3-phosphorylcholine (platelet-activating factor), of its enantiomer and of some analogous compounds. *Helv. Chim. Acta.* 65: 1059–1084.

Hope, M. J., D. C. Walker, and P. R. Cullis. 1983. Ca^{2+}- and pH-induced fusion of small unilamellar vesicles consisting of phosphatidylethanolamine and negatively charged phospholipids: a freeze fracture study. *Biochem. Biophys. Res. Commun.* 110:15–22.

Huang, C., and J. T. Mason. 1986. Structure and properties of mixed-chain phospholipid assemblies. *Biochim. Biophys. Acta.* 864:423–470

Huang, C., J. T. Mason, F. A. Stephensen, and I. W. Levin. 1984. Raman and ^{31}P NMR spectroscopic identification of a highly ordered lamellar phase in aquous dispersions of 1-stearoyl-2-acetyl-sn-glycerol-3-phosphorylcholine. *J. Phys. Chem.* 88:6454–6458.

Huang, C., J. T. Mason, F. A. Stephensen, and I. W. Levin. 1986. Polymorphic phase behavior of platelet-activating factor. *Biophys. J.* 49: 587–595.

Hui, S. W., and C. Huang. 1986. X-ray diffraction evidence for fully interdigitated bilayers of 1-stearoyl-lyso-phosphatidylcholine. *Biochemistry.* 25:1330–1335.

Hui, S. W., J. T. Mason, and C. Huang. 1984. Acyl chain interdigitation in saturated mixed-chain phosphatidyl-choline bilayer dispersions. *Biochemistry.* 23:5570–5577.

Mangroo, D., and G. E. Gerber. 1988. Phospholipid synthesis: effects of solvents and catalysts on acylation. *Chem. Phys. Lipids.* 48:99–108.

Mason, J. T., A. V. Broccoli, and C. Huang. 1981. A method for the synthesis of isomerically pure saturated mixed-chain phosphatidylcholines. *Anal. Biochem.* 113:96–101.

Mattai, J., and G. G. Shipley. 1986. The kinetics of formation and structure of the low-temperature phase of 1-stearoyl-lysophosphatidylcholine. *Biochim. Biophys. Acta.* 859:257–265.

Mattai J., P. K. Sripada, and G. G. Shipley. 1987. Mixed-chain phosphatidylcholine bilayers: Structure and properties. *Biochemistry.* 26: 3287–3297.

McIntosh, T. J., S. A. Simon, J. C. Ellington, and N. A. Porter. 1984. New structural model for mixed-chain phosphatidylcholine bilayers. *Biochemistry.* 23:4038–4044.

Meneses, P., and T. Glonek. 1988. High resolution ^{31}P NMR of extracted phospholipids. *J. Lipid Res.* 29:679–689.

Nagle, J. F., and D. A. Wilkinson. 1978. Lecithin bilayers; Density measurements and molecular interactions. *Biophys. J.* 23:159–175.

Patel, K. M., and J. T. Sparrow. 1979. Phase transfer catalysis: reaction of 4-bromopyridine with cyclic secondary amines. *Syn. Commun.* 9: 251–253.

Rand, R. P., and V. A. Parsegian. 1989. Hydration forces between phospholipids bilayers. *Biochim. Biophys. Acta.* 988:351–376.

Rand, R. P., N. L. Fuller, S. M. Gruner, and V. A. Parsegian. 1990. Membrane curvature, lipid segregation, and structural transitions for phospholipids under dual-solvent stress. *Biochemistry.* 29:76–87.

Reiss-Husson, F. 1967. Structure des phases liquide-cristallines de differents phospholipides, monoglycerides, sphingolipides, anhydres ou en presence d'eau. *J. Mol. Biol.* 25:363–382.

Satouchi, K., M. Oda, K. Yasunga, and K. Saito. 1985. Evidence for production of 1-acyl-2-acetyl-sn-glyceryl-3-phosphorylcholine concomitantly with platelet-activating factor. *Biochem. Biophys. Res. Commun.* 128:1409–1417.

Satouchi, K., M. Oda, and K. Saito. 1987. 1-Acyl-2-acetyl-sn-glycero-3-phosphocholine from stimulated polymorphonuclear leukocytes. *Lipids.* 22:285–287.

Shah, J., P. K. Sripada, and G. G. Shipley. 1990. Structure and properties of mixed-chain phosphatidylcholine bilayers. *Biochemistry.* 29: 4254–4262.

Shannon, C. E. 1949. Communication in the presence of noise. *Proc. Inst. Radio Eng. N. Y.* 37:10–21.

Tardieu, A., V. Luzzati, and F. C. Reman. 1973. Structure and polymorphism of the hydrocarbon chains of lipids: a study of lecithin-water phases. *J. Mol. Biol.* 75:711–733.

Tence, M., E. Coeffier, F. Heymans, J. Polonsky, J. J. Godfroid, and J. Benveniste. 1981. Structural analogs of platelet-activating factor (PAF-acether). *Biochimie.* 63:723–727.

Tokumura, A., T. Kume, K. Fukuzawa, and H. Tsukatani. 1981. Cardiovascular effects of lysophosphatidic acid and its structural analogs in rats. *J. Pharmacol. Exp. Ther.* 219:219–224.

Tokumura, A., T. Maruyama, K. Fukuzawa, and H. Tsukatani. 1985. Effects of lysophosphatidic acids and their structural analogs on arterial blood pressure of cats. *Arzneim.-Forsch.* 35:587–592.

Wu, W., and C. Huang. 1983. Kinetic studies of the micellar to lamellar phase transition of 1-stearoyl-lysophosphatidylcholine dispersions. *Biochemistry.* 22:5068–5073.

Wu, W., C. Huang, T. G. Conley, R. B. Martin, and I. W. Levin. 1982. Lamellar-micellar transition of 1-stearoyllyso-phosphatidylcholine assemblies in excess water. *Biochemistry.* 21:5957–5961.

Wu, W., F. A. Stephenson, J. T. Mason, and C. Huang. 1984. A nuclear magnetic resonance spectroscopic investigation of the headgroup motion of lysophospholipids in bilayers. *Lipids.* 19:68–71.

Zettlemoyer, A. C. 1969. Nucleation. A. C. Zettlemoyer, editor. Marcel Dekker Inc., New York.